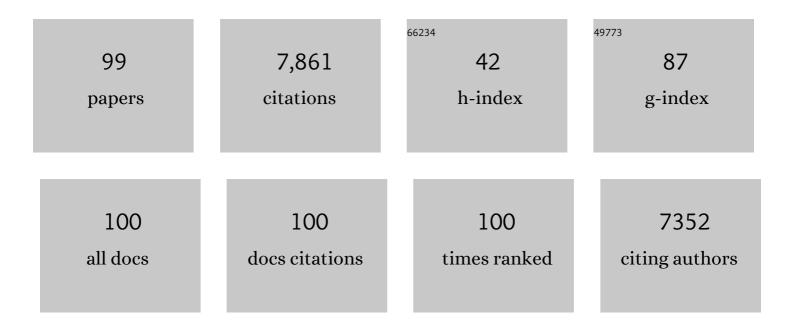
List of Publications by Year in descending order

Source: https://exaly.com/author-pdf/5738255/publications.pdf Version: 2024-02-01



#	Article	IF	CITATIONS
1	Solar-driven interfacial evaporation. Nature Energy, 2018, 3, 1031-1041.	19.8	1,347
2	Temperature effect and thermal impact in lithium-ion batteries: A review. Progress in Natural Science: Materials International, 2018, 28, 653-666.	1.8	745
3	A Bioinspired, Reusable, Paperâ€Based System for Highâ€Performance Largeâ€Scale Evaporation. Advanced Materials, 2015, 27, 2768-2774.	11.1	698
4	Bioâ€Inspired Evaporation Through Plasmonic Film of Nanoparticles at the Air–Water Interface. Small, 2014, 10, 3234-3239.	5.2	418
5	Coupling Interface Constructions of MoS ₂ /Fe ₅ Ni ₄ S ₈ Heterostructures for Efficient Electrochemical Water Splitting. Advanced Materials, 2018, 30, e1803151.	11.1	230
6	Bioinspired Engineering of Thermal Materials. Advanced Materials, 2015, 27, 428-463.	11.1	225
7	Bioinspired Multifunctional Paper-Based rGO Composites for Solar-Driven Clean Water Generation. ACS Applied Materials & Interfaces, 2016, 8, 14628-14636.	4.0	223
8	Bioinspired Bifunctional Membrane for Efficient Clean Water Generation. ACS Applied Materials & Interfaces, 2016, 8, 772-779.	4.0	187
9	Paper-based membranes on silicone floaters for efficient and fast solar-driven interfacial evaporation under one sun. Journal of Materials Chemistry A, 2017, 5, 16359-16368.	5.2	158
10	In Situ Vertical Growth of Fe–Ni Layered Double-Hydroxide Arrays on Fe–Ni Alloy Foil: Interfacial Layer Enhanced Electrocatalyst with Small Overpotential for Oxygen Evolution Reaction. ACS Energy Letters, 2018, 3, 2357-2365.	8.8	150
11	Solar steam generation: Steam by thermal concentration. Nature Energy, 2016, 1, .	19.8	148
12	Dynamic tuning of optical absorbers for accelerated solar-thermal energy storage. Nature Communications, 2017, 8, 1478.	5.8	145
13	Efficient Solar-Thermal Energy Harvest Driven by Interfacial Plasmonic Heating-Assisted Evaporation. ACS Applied Materials & Interfaces, 2016, 8, 23412-23418.	4.0	144
14	The impact of surface chemistry on the performance of localized solar-driven evaporation system. Scientific Reports, 2015, 5, 13600.	1.6	140
15	In Situ Environmental TEM in Imaging Gas and Liquid Phase Chemical Reactions for Materials Research. Advanced Materials, 2016, 28, 9686-9712.	11.1	124
16	Solar-driven interfacial desalination for simultaneous freshwater and salt generation. Desalination, 2020, 484, 114423.	4.0	121
17	Magnetically-accelerated large-capacity solar-thermal energy storage within high-temperature phase-change materials. Energy and Environmental Science, 2019, 12, 1613-1621.	15.6	110
18	Platinumâ€Based Nanowires as Active Catalysts toward Oxygen Reduction Reaction: In Situ Observation of Surfaceâ€Diffusionâ€Assisted, Solid‣tate Oriented Attachment. Advanced Materials, 2017, 29, 1703460.	11.1	102

#	Article	IF	CITATIONS
19	Floating rGO-based black membranes for solar driven sterilization. Nanoscale, 2017, 9, 19384-19389.	2.8	92
20	Infrared Detection Based on Localized Modification of <i>Morpho</i> Butterfly Wings. Advanced Materials, 2015, 27, 1077-1082.	11.1	90
21	Nanoscale kinetics of asymmetrical corrosion in core-shell nanoparticles. Nature Communications, 2018, 9, 1011.	5.8	87
22	All-in-one polymer sponge composite 3D evaporators for simultaneous high-flux solar-thermal desalination and electricity generation. Nano Energy, 2022, 93, 106882.	8.2	87
23	Neighboring Pt Atom Sites in an Ultrathin FePt Nanosheet for the Efficient and Highly CO-Tolerant Oxygen Reduction Reaction. Nano Letters, 2018, 18, 5905-5912.	4.5	84
24	Form-Stable Solar Thermal Heat Packs Prepared by Impregnating Phase-Changing Materials within Carbon-Coated Copper Foams. ACS Applied Materials & Interfaces, 2019, 11, 3417-3427.	4.0	83
25	Plasmonic-Enhanced Oxygen Reduction Reaction of Silver/Graphene Electrocatalysts. Nano Letters, 2019, 19, 1371-1378.	4.5	74
26	High-Efficiency Superheated Steam Generation for Portable Sterilization under Ambient Pressure and Low Solar Flux. ACS Applied Materials & Interfaces, 2019, 11, 18466-18474.	4.0	69
27	Rapid Charging of Thermal Energy Storage Materials through Plasmonic Heating. Scientific Reports, 2014, 4, 6246.	1.6	66
28	Enhancing Localized Evaporation through Separated Light Absorbing Centers and Scattering Centers. Scientific Reports, 2015, 5, 17276.	1.6	63
29	Bioinspired roll-to-roll solar-thermal energy harvesting within form-stable flexible composite phase change materials. Journal of Materials Chemistry A, 2020, 8, 20970-20978.	5.2	62
30	All-Day Freshwater Harvesting through Combined Solar-Driven Interfacial Desalination and Passive Radiative Cooling. ACS Applied Materials & Interfaces, 2020, 12, 47612-47622.	4.0	60
31	Three-Dimensional Porous Solar-Driven Interfacial Evaporator for High-Efficiency Steam Generation under Low Solar Flux. ACS Omega, 2019, 4, 3546-3555.	1.6	58
32	Synthesis of Liquid Gallium@Reduced Graphene Oxide Core–Shell Nanoparticles with Enhanced Photoacoustic and Photothermal Performance. Journal of the American Chemical Society, 2022, 144, 6779-6790.	6.6	57
33	Biotemplated <i>Morpho</i> Butterfly Wings for Tunable Structurally Colored Photocatalysts. ACS Applied Materials & Interfaces, 2018, 10, 4614-4621.	4.0	54
34	An open thermo-electrochemical cell enabled by interfacial evaporation. Journal of Materials Chemistry A, 2019, 7, 6514-6521.	5.2	52
35	Strong Electronic Interaction of Amorphous Fe ₂ O ₃ Nanosheets with Singleâ€Atom Pt toward Enhanced Carbon Monoxide Oxidation. Advanced Functional Materials, 2019, 29, 1904278.	7.8	51
36	Fabrication and performance evaluation of flexible heat pipes for potential thermal control of foldable electronics. Applied Thermal Engineering, 2016, 95, 445-453.	3.0	49

WEN SHANG

#	Article	IF	CITATIONS
37	Patterned Surfaces for Solar-Driven Interfacial Evaporation. ACS Applied Materials & Interfaces, 2019, 11, 7584-7590.	4.0	49
38	Photothermally Enabled Pyro-Catalysis of a BaTiO ₃ Nanoparticle Composite Membrane at the Liquid/Air Interface. ACS Applied Materials & amp; Interfaces, 2018, 10, 21246-21253.	4.0	48
39	Strain-Induced Corrosion Kinetics at Nanoscale Are Revealed in Liquid: Enabling Control of Corrosion Dynamics of Electrocatalysis. CheM, 2020, 6, 2257-2271.	5.8	48
40	Stably dispersed high-temperature Fe ₃ O ₄ /silicone-oil nanofluids for direct solar thermal energy harvesting. Journal of Materials Chemistry A, 2016, 4, 17503-17511.	5.2	45
41	Enhancing the Photocatalytic Hydrogen Evolution Performance of a Metal/Semiconductor Catalyst through Modulation of the Schottky Barrier Height by Controlling the Orientation of the Interface. ACS Applied Materials & Mary Interfaces, 2017, 9, 12494-12500.	4.0	45
42	Flexible heat pipes with integrated bioinspired design. Progress in Natural Science: Materials International, 2015, 25, 51-57.	1.8	43
43	Vapor-Enabled Propulsion for Plasmonic Photothermal Motor at the Liquid/Air Interface. Journal of the American Chemical Society, 2017, 139, 12362-12365.	6.6	43
44	Reconsidering the Benchmarking Evaluation of Catalytic Activity in Oxygen Reduction Reaction. IScience, 2020, 23, 101532.	1.9	42
45	Bioinspired Temperature Regulation in Interfacial Evaporation. Advanced Functional Materials, 2020, 30, 1910481.	7.8	42
46	Pyroelectric Synthesis of Metal–BaTiO ₃ Hybrid Nanoparticles with Enhanced Pyrocatalytic Performance. ACS Sustainable Chemistry and Engineering, 2019, 7, 2602-2609.	3.2	41
47	Stability of single-atom catalysts for electrocatalysis. Journal of Materials Chemistry A, 2022, 10, 5835-5849.	5.2	40
48	Substrateless Welding of Self-Assembled Silver Nanowires at Air/Water Interface. ACS Applied Materials & Interfaces, 2016, 8, 20483-20490.	4.0	39
49	Bioinspired Infrared Sensing Materials and Systems. Advanced Materials, 2018, 30, e1707632.	11.1	36
50	Heterostructure of ZnO Nanosheets/Zn with a Highly Enhanced Edge Surface for Efficient CO ₂ Electrochemical Reduction to CO. ACS Applied Materials & Interfaces, 2021, 13, 10837-10844.	4.0	33
51	Noncontact human-machine interaction based on hand-responsive infrared structural color. Nature Communications, 2022, 13, 1446.	5.8	33
52	Temperature-Induced Coalescence of Colliding Binary Droplets on Superhydrophobic Surface. Scientific Reports, 2014, 4, 4303.	1.6	32
53	Erythritol impregnated within surface-roughened hydrophilic metal foam for medium-temperature solar-thermal energy harvesting. Energy Conversion and Management, 2020, 222, 113241.	4.4	32
54	Integrating plasmonic nanostructures with natural photonic architectures in Pd-modified <i>Morpho</i> butterfly wings for sensitive hydrogen gas sensing. RSC Advances, 2018, 8, 32395-32400.	1.7	31

#	Article	IF	CITATIONS
55	Butterfly Wing Hears Sound: Acoustic Detection Using Biophotonic Nanostructure. Nano Letters, 2019, 19, 2627-2633.	4.5	29
56	Vertical segregation in the self-assembly of nanoparticles at the liquid/air interface. Nanoscale, 2014, 6, 14662-14666.	2.8	25
57	Ternary Pt–Pd–Ag alloy nanoflowers for oxygen reduction reaction electrocatalysis. CrystEngComm, 2017, 19, 6964-6971.	1.3	23
58	Design of Highly Durable Coreâ^'Shell Catalysts by Controlling Shell Distribution Guided by In‣itu Corrosion Study. Advanced Materials, 2021, 33, e2101511.	11.1	21
59	Clean water generation with switchable dispersion of multifunctional Fe3O4-reduced graphene oxide particles. Progress in Natural Science: Materials International, 2018, 28, 422-429.	1.8	20
60	Structural evolution of Pt-based oxygen reduction reaction electrocatalysts. Chinese Journal of Catalysis, 2022, 43, 47-58.	6.9	20
61	Subtractive Structural Modification of <i>Morpho</i> Butterfly Wings. Small, 2015, 11, 5705-5711.	5.2	17
62	Electrically Driven Interfacial Evaporation for High-Efficiency Steam Generation and Sterilization. ACS Omega, 2019, 4, 16603-16611.	1.6	17
63	Atomistic Imaging of Competition between Surface Diffusion and Phase Transition during the Intermetallic Formation of Faceted Particles. ACS Nano, 2021, 15, 5284-5293.	7.3	17
64	Galliumâ€Based Liquid Metal Composites with Enhanced Thermal and Electrical Performance Enabled by Structural Engineering of Filler. Advanced Engineering Materials, 2022, 24, 2101678.	1.6	16
65	Facile Approach to Enhance Electrical and Thermal Performance of Conducting Polymer PEDOT:PSS Films via Hot Pressing. ACS Applied Materials & Interfaces, 2022, 14, 10605-10615.	4.0	16
66	Evaporation: Bioâ€Inspired Evaporation Through Plasmonic Film of Nanoparticles at the Air–Water Interface (Small 16/2014). Small, 2014, 10, 3233-3233.	5.2	14
67	In Situ Transmission Electron Microscopy Study of Nanocrystal Formation for Electrocatalysis. ChemNanoMat, 2019, 5, 1439-1455.	1.5	14
68	Ethylene glycol-based solar-thermal fluids dispersed with reduced graphene oxide. RSC Advances, 2019, 9, 10282-10288.	1.7	14
69	Bubbleâ€Enabled Underwater Motion of a Lightâ€Driven Motor. Small, 2019, 15, e1804959.	5.2	14
70	Selfâ€Assembly in Hopperâ€&haped Crystals. Advanced Functional Materials, 2020, 30, 1908108.	7.8	14
71	Human hand as a powerless and multiplexed infrared light source for information decryption and complex signal generation. Proceedings of the National Academy of Sciences of the United States of America, 2021, 118, .	3.3	14
72	Construction of 3D Conductive Network in Liquid Gallium with Enhanced Thermal and Electrical Performance. Advanced Materials Technologies, 2022, 7, 2100970.	3.0	14

#	Article	IF	CITATIONS
73	Rapid one-step scalable microwave synthesis of Ti ₃ C ₂ T _{<i>x</i>} MXene. Chemical Communications, 2021, 57, 12611-12614.	2.2	14
74	Manipulation of Electron Transfer between Pd and TiO ₂ for Improved Electrocatalytic Hydrogen Evolution Reaction Performance. ACS Applied Materials & Interfaces, 2020, 12, 27037-27044.	4.0	13
75	Facets Matching of Platinum and Ferric Oxide in Highly Efficient Catalyst Design for Low-Temperature CO Oxidation. ACS Applied Materials & Interfaces, 2018, 10, 15322-15327.	4.0	12
76	Self-propelled rotation of paper-based Leidenfrost rotor. Applied Physics Letters, 2019, 114, .	1.5	12
77	Self-powered infrared detection using a graphene oxide film. Journal of Materials Chemistry A, 2020, 8, 9248-9255.	5.2	12
78	Controllable assembly of Pd nanosheets: a solution for 2D materials storage. CrystEngComm, 2017, 19, 3439-3444.	1.3	12
79	Coalescence, Spreading, and Rebound of Two Water Droplets with Different Temperatures on a Superhydrophobic Surface. ACS Omega, 2019, 4, 17615-17622.	1.6	9
80	Self-dispersible graphene quantum dots in ethylene glycol for direct absorption-based medium-temperature solar-thermal harvesting. RSC Advances, 2020, 10, 45028-45036.	1.7	8
81	Effectively Tuning the Ratio of CO and H ₂ into Syngas through CO ₂ Electrochemical Reduction over a Wide Potential Range on a ZnO Nanosheet via Ni Doping. ACS Applied Energy Materials, 2022, 5, 5531-5539.	2.5	8
82	Paste-like recyclable Ga liquid metal phase change composites loaded with miscible Ga2O3 particles for transient cooling of portable electronics. Applied Thermal Engineering, 2022, 213, 118766.	3.0	8
83	Coupling effects in 3D plasmonic structures templated by <i>Morpho</i> butterfly wings. Nanoscale, 2018, 10, 533-537.	2.8	7
84	Butterfly Wing Inspired High Performance Infrared Detection with Spectral Selectivity. Advanced Optical Materials, 2020, 8, 1901647.	3.6	7
85	Boosting Oxygen and Peroxide Reduction Reactions on PdCu Intermetallic Cubes. ChemElectroChem, 2020, 7, 2614-2620.	1.7	7
86	Chemo- and stereospecific solid-state dimerization of lithium trans-2-butenoate and lithium trans-2-butenoate formamide solvate. CrystEngComm, 2011, 13, 4339.	1.3	6
87	Transparent nanofluids with high thermal conductivity for improved convective thermal management of optoelectronic devices. Experimental Heat Transfer, 2022, 35, 183-195.	2.3	6
88	Unzipping Carbon Nanotube Bundles through NHâ^'Ï€ Stacking for Enhanced Electrical and Thermal Transport. ACS Applied Materials & Interfaces, 2021, 13, 28583-28592.	4.0	6
89	Bioinspired infrared detection using thermoresponsive hydrogel nanoparticles. Pure and Applied Chemistry, 2015, 87, 1029-1038.	0.9	4
90	Pyroelectric synthesis of Au/Pt bimetallic nanoparticles–BaTiO ₃ hybrid nanomaterials. RSC Advances, 2020, 10, 22616-22621.	1.7	3

#	Article	IF	CITATIONS
91	The impact of surface chemistry on the interfacial evaporation-driven self-assembly of thermoplasmonic gold nanoparticles. Nanoscale, 2021, 13, 20521-20530.	2.8	3
92	A Nonâ€₽t Electronically Coupled Semiconductor Heterojunction for Enhanced Oxygen Reduction Electrocatalytic Property. ChemistrySelect, 2019, 4, 5264-5268.	0.7	2
93	Light-Driven Nanodroplet Generation Using Porous Membranes. Nano Letters, 2020, 20, 7874-7881.	4.5	2
94	Chemo- and Stereospecific Solid-State Thermal Dimerization of Sodium trans-2-Butenoate and Î ³ -Ray-Induced Single-Crystal-to-Single-Crystal Dimerization of Hexaaquamagnesium trans-2-Butenoate Dihydrate: Both Give rel-(3S,4R)-1-Hexene-3,4-dicarboxylate but by Different Mechanisms. Stereospecific Î ³ -Ray-Induced Trimerization of Sodium trans-2-Butenoate. Crystal Growth and Design, 2021, 21, 663-682.	1.4	2
95	Bioinspired Color Change through Guided Reflection. Advanced Optical Materials, 2018, 6, 1800464.	3.6	1
96	Integration of Biological Components into Engineered Functional Systems. Matter, 2020, 3, 974-976.	5.0	1
97	Ethylene glycol nanofluids dispersed with monolayer graphene oxide nanosheet for high-performance subzero cold thermal energy storage. RSC Advances, 2021, 11, 30495-30502.	1.7	1
98	Pyroelectric Synthesis of the Siteâ€Specific Auâ€ZnO Nanorod Array. ChemistrySelect, 2021, 6, 11224-11230.	0.7	1
99	Hopper‧haped Crystals: Selfâ€Assembly in Hopper‧haped Crystals (Adv. Funct. Mater. 26/2020). Advanced Functional Materials, 2020, 30, 2070170.	7.8	0